

A Printed Crescent Patch Antenna for Ultrawideband Applications

Ntsanderh C. Azenui and H. Y. D. Yang

Abstract—A miniaturized crescent-shape microstrip antenna is proposed for ultrawideband (3–10 GHz) applications. The crescent antenna is evolved from an elliptical patch antenna by carving a circular hole inside symmetrically. The circular aperture introduces an additional antenna in-band resonance and provides wider bandwidth with more design flexibility. The radiation characteristics of this crescent antenna are investigated with full-wave electromagnetic simulations and compared with an elliptical antenna. A crescent antenna prototype that occupies only 60% area of the elliptical patch is fabricated and tested. Antenna pattern and impedance measurements show good performance over the 3–10 GHz band with consistent radiation patterns, low cross polarization, and a substantial gain. The design method is also described.

Index Terms—Disc monopole, patch antenna, printed circuits, ultrawideband.

I. INTRODUCTION

IEEE 802.15 standard utilizing the frequency spectrum from 3 to 10 GHz for high-data rate ultrawide band applications has attracted significant attention recently in wireless industry. High-performance miniaturized front-end printed circuit board antennas are essential in portable systems [1], [2]. There is an ever growing demand of reducing antenna area while maintaining or increasing bandwidth. The circular or elliptical shape monopole antennas are found to have sufficient 10 dB return-loss bandwidth for ultrawideband applications [3]–[12]. The antennas integrated on a printed circuit board can be viewed as a suspended monopole antenna collapsed on the substrate surface. Without a conductor on the back to form a resonator, it maintains the low- Q feature of a suspended antenna and is broadband. A 50- Ω trace extends into the antenna central arm and it requires a conductor backing to form a microstrip transmission line. The circular/elliptical patch antenna is in effect consisting of many crescent-shape wire antennas. The existence of many possible current modes explains the reason of such a broad antenna bandwidth. The current modes that could exist on a circular metal patch are in the form of higher order Bessel functions of the first kind, where the current is small at the center of the patch and mostly concentrated on its periphery.

Manuscript received August 29, 2006; revised December 20, 2006. This work was supported in part by the National Science Foundation under STTR Grant OII-0539198.

The authors are with the Department of Electrical and Computer Engineering, University of Illinois, Chicago, IL 60607 USA (e-mail: hyang@ece.uic.edu).

Color versions of one or more of the figures are available online at <http://ieeexplore.ieee.org>.

Digital Object Identifier 10.1109/LAWP.2007.891522

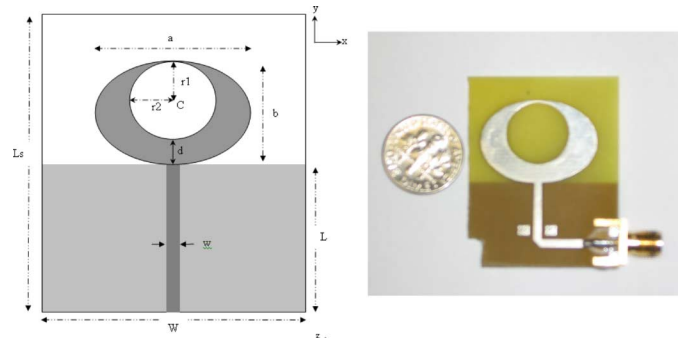


Fig. 1. Antenna structure and photograph of a crescent-shaped patch antenna.

In this letter, a novel miniaturized crescent-shape antenna is proposed that would significantly reduce the overall antenna area. The basic structure is an elliptical-shape patch with a symmetric elliptical aperture in it. The inner aperture area can be used for communication circuit components. A parametric study of the antenna return loss in terms of the major and minor axes of the elliptical aperture is presented through the use of the Ansoft high-frequency structure simulator (HFSS). The crescent antenna prototype is fabricated and tested. The measured radiation pattern, gain, and returned loss are characterized and compared with those of an elliptical patch. The design procedures and formulas are also discussed.

II. THE DESIGN OF A CRESCENT-SHAPED PRINTED CIRCUIT PATCH ANTENNA

The crescent patch antenna for ultrawideband communications proposed in this letter is shown in Fig. 1. The elliptical patch is designed with a major axis $a = 27.0$ mm, and a minor axis $b = 18.0$ mm (ellipticity ratio $a/b = 1.5$), from which a circular region of radius $r_1 = r_2 = 7.0$ mm is carved out. The center of this circular region is displaced by 2.0 mm above the center of the outer ellipse. The idea of cutting out a circular region derives from the examination of the current distribution of the elliptical patch antenna. It is observed that the currents on the elliptical patch radiator at all frequencies are mostly concentrated on its periphery, with very low current density toward its center. The initial design parameters are based on formulas described in Section III. Both Zeland IE3D and Ansoft HFSS simulations are used to optimize the design.

The crescent patch prototype is printed on an FR4 material of relative permittivity $\epsilon_r = 4.2$ and of loss tangent of 0.01, with no ground plane directly underneath it. The substrate thickness is $h = 0.762$ mm ($= 30$ mil). The antenna is fed by a 50- Ω microstrip transmission line which consists of a trace of width $w = 1.524$ mm (60 mil), printed on the surface of the substrate

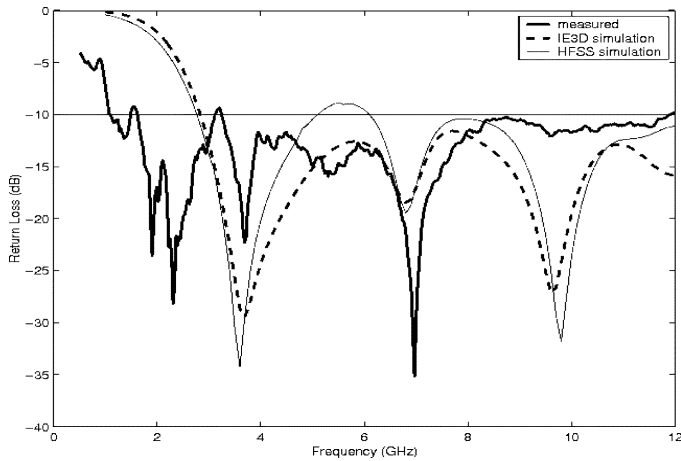


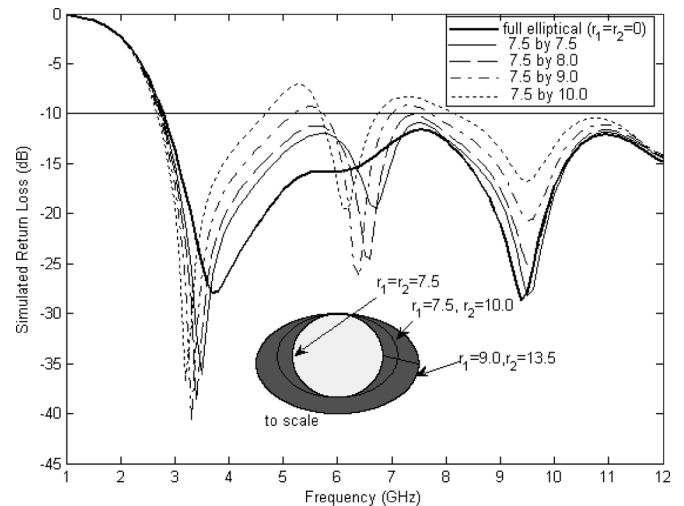
Fig. 2. Return loss characteristics of crescent shaped patch antenna.

that is partially backed by a ground plane. The ground plane has dimensions $W = 45$ mm and $L = 21.5$ mm, and the length extension from the ground plane edge to the substrate edge is 29.5 mm ($L_s = 50$ mm). The actual ground plane length is insignificant to the antenna performance unless it is too small (as a radiator by itself). The antenna location relative to the substrate edge affects the antenna performance slightly. There is an overlap of $86 \mu\text{m}$ between the patch and the ground plane in the minor axis direction of the patch. This overlap region is used to fine tune the impedance. All conducting elements of the antenna are realized with a half ounce of copper.

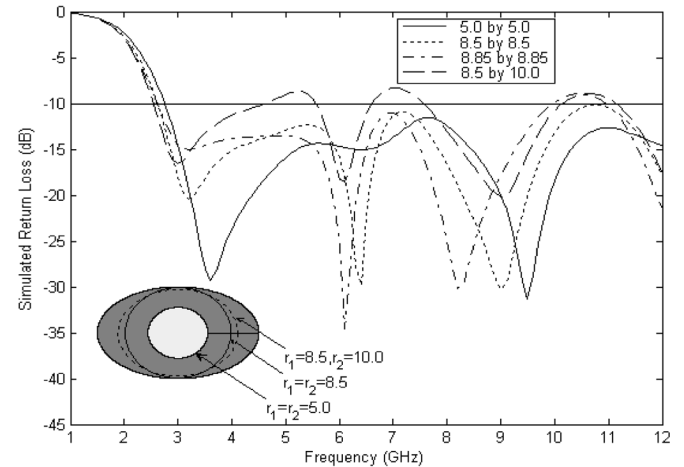
A. Antenna Return Loss

Numerical simulations and measurements were conducted on the crescent-shaped patch antenna. The simulations and optimizations are based on Ansoft HFSS and an HP8510C network analyzer and on-surface probes are used for the impedance measurements. Its return loss characteristics are presented in Fig. 2, and show that it has an impedance bandwidth for return loss less than -10 dB from 2.7–12 GHz. In addition, there is good agreement between the measured and simulated return loss results from 2.8 to 8.0 GHz, but discrepancies exist between the two beyond 8.0 GHz. One reason for the latter could be that the simulations do not correctly model substrate losses—assumed to remain constant—above 8.0 GHz. The discrepancy in the low frequencies (below 3 GHz) is mostly due to the small ground plan and substrate.

Parametric studies of the effect of the inner-hole (r_1 and r_2 in Fig. 1) on the return loss (antenna impedance) using HFSS are shown in Fig. 3. For comparison, the case without the inner hole is also shown. It is observed from Fig. 3(a) and (b) that when both of r_1 and r_2 are less than 7.0 mm (ellipse major and minor axes: 27 and 18 mm), the return loss of the crescent antenna (also true for other radiation characteristics) are nearly identical to those of the full elliptical antenna. However, when they are both greater than 7 mm, an additional resonance appears. A larger inner hole corresponds to a lower second resonant frequency. This is due to the fact that for a larger the hole, the current path along the inner periphery is longer, and that corresponds to a longer monopole wire. Half of the perimeter of the cutout hole is



(a)



(b)

Fig. 3. Parametric studies of effect of r_1 and r_2 on the return loss of crescent antenna.

a resonant length at the intermediate resonance frequency. The limits of r_1 and r_2 for which the crescent antenna has an additional resonance while preserving the impedance bandwidth as compared to the full elliptical antenna can be found from Fig. 3 to be approximately $7.0 \text{ mm} < r_1 < 8.7 \text{ mm}$ and $7.0 \text{ mm} < r_2 < 8.7 \text{ mm}$ for the present design. An upper limit of 8.7 mm for r_1 is interesting. It means that the crescent antenna still exhibits ultrawideband performance even when the inner circle is approaching the edge of the ellipse (d in Fig. 1 is 0.3 mm). If the inner hole is too large, the first two resonances merge and, thus, degrade the impedance match. Also, it is found that the wideband property seems to be better preserved by a circular rather than an elliptical hole.

B. Current Modes

Through a numerical study of the vector current distribution on the antenna prototype ($r_1 = r_2 = 7.0$ mm), three characteristic current modes are found to exist on the crescent patch over the bandwidth from 3.0 to 10.0 GHz. Using Fig. 2 as a reference, each current mode is dominant at each antenna resonance, 3.7,

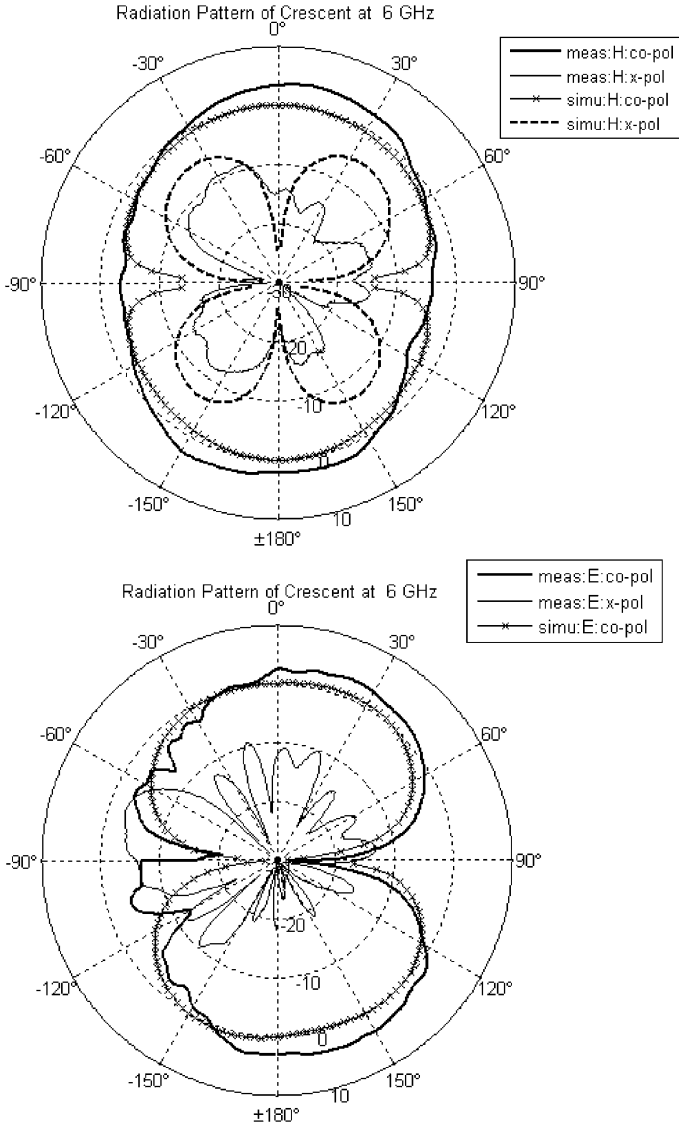


Fig. 4. Measured and simulated radiation patterns of a crescent antenna at 6 GHz.

6.8, and 9.6 GHz, respectively. A full-wave simulation of the elliptical microstrip disc modes (with a ground plate) shows that the resonant frequencies are at 5.5 and 10.6 GHz (the crescent disc modes have similar resonant frequencies). It is seen that for the antenna mode, the crescent (or ellipse) patch is more like a resonant curved half-wave length dipole, rather than a low Q factor disc resonator.

C. Radiation Patterns

Simulated and measured results of the radiation patterns of the crescent antenna ($r_1 = r_2 = 7.0$ mm) and the corresponding full elliptical antenna are presented in Figs. 4 and 5, respectively. The results include copolarization and cross polarization in the $E(yz)$ -plane and the $H(xz)$ -plane (Fig. 1). Although only the results at 6 GHz are shown, the patterns resemble a donut shape with an approximately omnidirectional H -plane pattern and a figure of eight pattern in the E -plane up to

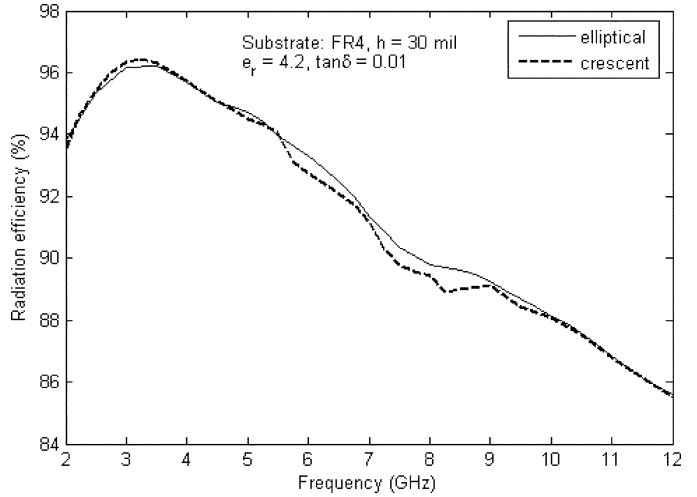


Fig. 5. Comparison of the simulated radiation efficiency of the elliptical and crescent antennas.

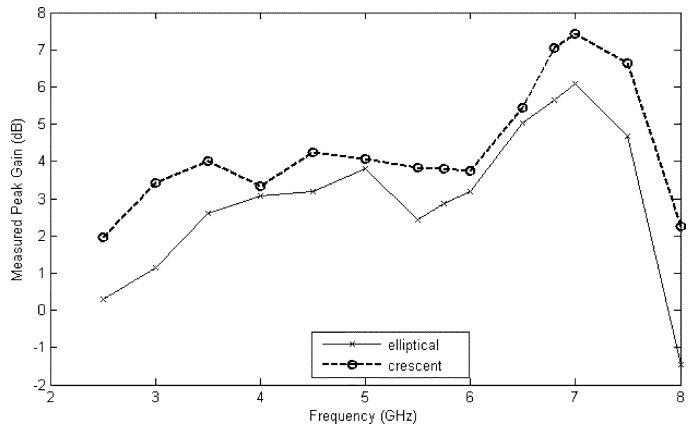


Fig. 6. Comparison of the measured peak gain of the elliptical and crescent antennas.

8 GHz. As the frequency increases beyond 8.0 GHz, however, and more high-order current modes are excited, the radiation pattern of the antenna becomes more directional; with the deformations introduced to the pattern appearing mostly as cross polarization in the H -plane, and resulting in tilting the main beam away from the broadside direction in the E -plane. Simulations results show a cross polarization in the E -plane of less than -30 dB for all frequencies although the measurements are slightly higher. The radiation patterns of the crescent antenna and the elliptical antenna are found similar. The measurement and simulation results agree fairly well.

The computed radiation efficiency of both the elliptical antenna and the crescent antenna is shown in Fig. 5. The comparison shows very close radiation efficiency throughout the whole 3–10 GHz band. This observation further validates the theory that most currents are on the edge of the ellipse and the cutout has insignificant effect on power loss on the conductor and substrate. However, the crescent antenna shows a slightly lower efficiency in the midband where there is a resonant mode with current crowded on the inner edge. This is due to the fact that there is a higher inner current density at the edge of the cutout hole and the conductor loss is higher for the crescent antenna.

Fig. 6 shows a comparison of measured peak antenna gain between the full elliptical antenna and the crescent antenna. It is found that the crescent antenna has a slightly higher peak gain throughout the entire band while maintaining similar efficiency (Fig. 5).

III. DESIGN FORMULAS FOR AN ELLIPTICAL PATCH ANTENNA

Although the prototype design is based on full-wave HFSS simulations, simple analytic formulas can be derived to provide an initial design and insight. Due to the fact that most current is concentrated on periphery, it is as if there is a wire antenna circulating around the ellipse (or circle). For ultrawide band design, the first resonant frequency should be slightly higher than the lower band boundary. The length of the ellipse perimeter should be around one wavelength long at the lowest in-band frequency (two half-wave length wires in parallel fed symmetrically). Practically, this frequency should be lower than 3 GHz in ultrawide band application to compensate for the environment variation.

For an ellipse of a major axis \mathbf{a} and a minor axis \mathbf{b} , the perimeter is given by

$$p = 2\mathbf{a}E(\mathbf{e}) \quad (1)$$

where $E(\mathbf{e})$ is a complete elliptic integral of the second kind with elliptic modulus \mathbf{e} , the eccentricity.

$$\mathbf{e} = \sqrt{1 - \left(\frac{\mathbf{b}}{\mathbf{a}}\right)^2}. \quad (2)$$

This can be computed numerically using Matlab. For the crescent and the elliptical antenna, the perimeter of the outer ellipse should be close to one wavelength of the average medium. If the lowest frequency in the impedance bandwidth of the antenna is f_L (GHz) and the effective permittivity of the medium of radiation can be approximated by

$$\epsilon_{\text{eff}} \approx \frac{(\epsilon_r + 1)}{2} \quad (3)$$

then

$$f_L = \frac{300}{p\sqrt{\epsilon_{\text{eff}}}} \quad (4)$$

where the perimeter unit is in millimeters. In the present design, $\mathbf{a} = 27$ mm and $\mathbf{b} = 18$ mm, $p = 71.4$ mm and $f_L \approx 2.6$ GHz. The full-wave HFSS simulation in Fig. 2 shows $f_L \approx 2.7$ GHz.

Comparing the results of the above computations, it is apparent that for both the crescent patch antenna and the elliptical antenna, the longest current path on the patch (or, equivalently, half of the perimeter of the patch) should be approximately half of the wavelength at the lowest frequency of

the antenna in-band. Further simulation shows that the optimum ellipticity \mathbf{a}/\mathbf{b} is about 1.5 for the crescent patch antenna in terms of the overall area and the lowest in-band frequency.

For practical applications in ultrawide band systems, the inner hole of the crescent can be used for RF circuits without affecting much of the antenna operation. The overall crescent antenna area could be reduced by 40% as compared to a full elliptical patch.

IV. CONCLUSION

A crescent shape monopole antenna was proposed for ultrawide band communications in the 3–10 GHz band. Parametric studies of the antenna characteristics were presented, and the radiation properties of an antenna prototype were discussed and compared with those of the full elliptical antenna. The crescent antenna prototype is found similar in radiation properties to the full elliptical antenna, but with 40% reduction in area (60% of the ellipse area). The characteristic current modes on the crescent antenna are identified and provide insights into the antenna properties. Finally, design formulas are given relating the lowest frequency in its operational band to the outer perimeter of the antenna.

REFERENCES

- [1] C. Soras, M. Karaboikis, G. Tsachtsiris, and V. Makios, "Analysis and design of an inverted-F antenna printed on a PCMCIA card for the 2.4 GHz ISM band," *IEEE Antennas Propag. Mag.*, vol. 44, no. 1, pp. 37–44, Feb. 2002.
- [2] H. Y. D. Yang, "Miniaturized printed wire antenna for wireless communications," *IEEE Antennas Wireless Propag. Lett.*, vol. 4, pp. 358–361, 2005.
- [3] S. Honda, M. Ito, H. Seki, and Y. Jingo, "A disc monopole antenna with 1:8 impedance bandwidth and omnidirectional radiation pattern," in *Proc. Int. Symp. Antennas Propag.*, Sapporo, Japan, Sep. 1992, pp. 145–149.
- [4] M. Hammoud *et al.*, "Matching the input impedance of a broadband disc monopole," *Electron. Lett.*, vol. 29, pp. 406–407, Feb. 1993.
- [5] N. P. Agrawal, G. Kumar, and K. P. Ray, "Wide-band planar monopole antennas," *IEEE Trans. Antennas Propag.*, vol. 46, pp. 29–295, Feb. 1998.
- [6] J. Powell and A. Chandrakasan, "Differential and single ended elliptical antennas for 3.1–10.6 GHz ultra wideband communication," in *IEEE APS Int. Symp.*, Jun. 2004, vol. 3, pp. 2935–2938.
- [7] H. G. Schantz, "Planar elliptical element ultra-wideband dipole antennas," in *IEEE APS Int. Symp.*, 2002, vol. 3.
- [8] M. J. Ammann and Z. J. Chen, "Wideband monopole antennas for multi-band wireless systems," *IEEE Antennas Propag. Mag.*, vol. 45, pp. 146–150, Apr. 2003.
- [9] C. Ying and Y. P. Zhang, "A planar antenna in LTCC for single-package ultrawide-band radio," *IEEE Trans. Antennas Propag.*, vol. 53, no. 9, pp. 3083–3093, Sep. 2005.
- [10] L. Jianxin, C. C. Chiau, C. Xiaodong, and C. G. Parini, "Study of a printed circular disc monopole antenna for UWB systems," *IEEE Trans. Antennas Propag.*, vol. 53, no. 2, pp. 3500–3504, Nov. 2005.
- [11] Z. N. Low, J. H. Cheong, and C. L. Law, "Low-cost PCB antenna for UWB applications," *IEEE Antennas Wireless Propag. Lett.*, vol. 4, pp. 237–239, 2005.
- [12] G. Lu, S. Mark, I. Korisch, L. Greenstein, and P. Spasojevic, "Diamond and rounded diamond antennas for ultra-wide-band communications," *IEEE Antennas Wireless Propag. Lett.*, vol. 3, pp. 249–252, 2004.